AIAA JOURNAL
Vol. 31, No. 9, September 1993

Periodic Vortex Shedding over Delta Wings

O. K. Rediniotis,* H. Stapountzis,† and D. P. Telionis‡
Virginia Polytechnic Institute and State University, Blacksburg, Virginia 24061

An experimental investigation was conducted on delta wings at high angles of attack. It was found that for angles of attack larger than 35 deg, periodic vortices are shed. Two modes of shedding were discovered: an alternate and a simultaneous. The first involves alternate shedding of vortices, much like shedding over two-dimensional bluff bodies. The second is dominated by simultaneous shedding of vortices, but its spatial characteristics are not yet well understood.

I. Introduction

ALL bluff bodies or flat surfaces at large angles of attack shed vortices alternately. Such problems have been investigated extensively by researchers interested in flow-induced vibrations, structural mechanics, wind engineering, automobile aerodynamics, and others. We list here only some recent review articles on these topics (Refs. 1–6). Barbie et al.[7] have also contributed in this area. So far, investigators of wing aerodynamics have not shown interest in the possibility that natural dynamic motions can develop over delta wings.

Several researchers[8–10] examined delta wings at angles of attack as high as 80 deg, but so far they have studied only averaged characteristics. The only contribution that indicated a true search for naturally evolving periodic phenomena is due to Ayoub and McLachlan.[11] Those authors observed a periodic motion of vortex breakdown but did not offer any evidence to support their observation.

The development of alternate periodic vortex shedding usually induces significant asymmetry on the pressure distribution over the surface of a body. Such asymmetries generated over a wing planform could have catastrophic consequences on the stability of an aircraft during high angle-of-attack maneuvers. In most practical cases, similar aerodynamic periodic oscillations are coupled with the motion of the aircraft and the interaction is known as wingrock,[12] but this phenomenon has been documented only for low angles of attack.

Alternate shedding of vortices will certainly induce oscillations on the attitude of the vehicle, but here we are interested in the pure aerodynamic phenomenon of sustained periodic flow oscillations over a fixed wing. The engineering implications of the present findings are obvious in the case of a dynamic maneuver that brings a wing to a very large angle of attack, where alternate vortex shedding is unavoidable. Periodic vortex shedding over slender axisymmetric bodies at high angles of attack has been documented in the literature.[13,14] However, in all of these studies the lines of separation are nearly parallel to each other, and therefore the vortex sheets on the two sides of the body interact with each other in an almost two-dimensional manner. The mechanism of vortex roll-up and shedding then results, with some minor modifications, to the classical Kármán street. Gaster and Ponsford[15] and later the present authors[16] and Klute et al.[17] explored the phenomenon of periodic vortex shedding over flat plates with nonparallel edges positioned normal to the flow. However, again the edges were nearly parallel, and except for the formation of cells, the wakes organized themselves in a nearly two-dimensional fashion. In the problem under discussion here, the edges form an angle of 30 deg, and moreover they are inclined with respect to the flow.

Preliminary findings on this problem were published by the present authors in a short Note.[18] The variation of the Strouhal number vs the angle of attack and the Reynolds number was partially investigated. The main thrust in the present effort is to explore the flowfield for organized natural oscillations and to identify their character. The existence of two different shedding modes (simultaneous and alternate) is now documented in terms of pairs of hot-wire signals. The angle-of-attack ranges in which each mode is present are investigated for the entire domain of shedding angles of attack ($35 \leq \alpha \leq 90$ deg). The orientation of the shed vortices with respect to the wing and their evolution in time are studied. Finally, flow visualization techniques are used to support the earlier findings.

II. Statement of the Problem

The flow over a delta wing at an angle of attack is dominated by the two leading-edge vortical structures. Those consist of two vortex sheets that emanate from the leading edges of the wing and roll up to form two axial vortices. The geometry is nearly conical, as long as the vortices develop over the surface of the wing. The axes of these vortices are along radii emanating from the apex. Farther downstream, the vortices turn and align themselves with the oncoming flow, as shown schematically in Fig. 1.

It is well known that if the sharp edges of a body are parallel to each other and normal to the flow, then the vortex sheets roll up and periodically detach from the body. This is, for example, the case for the flow over a flat plate with a very large aspect ratio, as shown schematically in Fig. 2. The phenomenon is well known as vortex shedding. This problem has been investigated by Roshko.[19] The present authors first repeated some of the classical tests that included testing of a large-aspect-ratio flat plate normal to the flow at different Reynolds numbers and then moved on to examine the case of

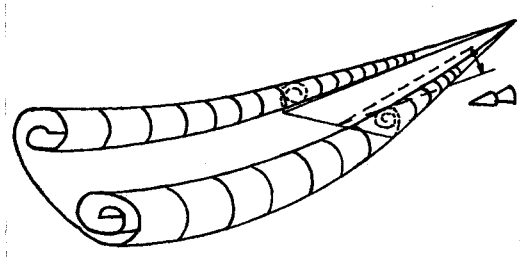

Fig. 1 Schematic of vortex sheets rolling over a delta wing at a moderate angle of attack.

Received April 8, 1991; revision received Sept. 1, 1992; accepted for publication Oct. 20, 1992.

*Graduate Student, Department of Engineering Science and Mechanics.

†Assistant Professor, Department of Engineering Science and Mechanics; on leave from Mechanical Engineering Department, University of Salonica, Greece.

‡Professor, Department of Engineering Science and Mechanics. Associate Fellow AIAA.

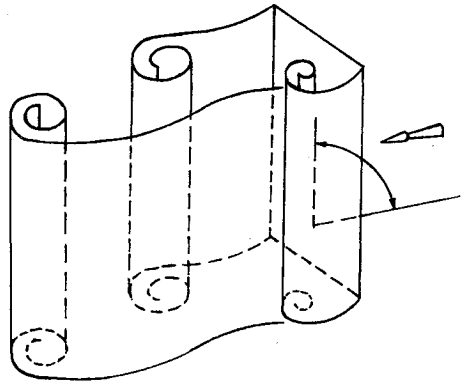

Fig. 2 Schematic of vortex sheets shedding over a flat plate positioned normal to the oncoming flow.

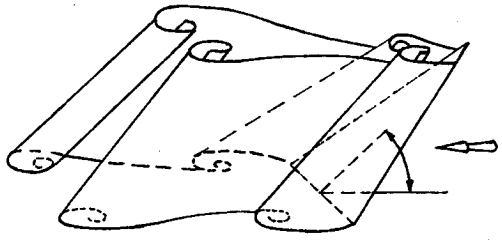

Fig. 3 Schematic of vortical structures shedding simultaneously over a delta wing at a large angle of attack.

vortex shedding over a flat plate at an angle of attack,[16] i.e., $\alpha < 90$ deg.

In nominally two-dimensional flows, like the one depicted in Fig. 2, the velocity vectors are contained in planes normal to the vectors of vorticity and therefore normal to the axis of the large-scale vortices. On the other hand, for the flow of Fig. 1, the dominant direction of the flow is nearly aligned with the direction of the axes of the vortices. In fact, in the core of the vortex, the velocity is along the axis of the vortex.

The terminology here requires some clarification. In aerodynamics, we often use the term "vortex shedding" to describe the departure of vorticity from a solid surface on which it was generated. For example, we use this term for vorticity leaving the tips of a finite wing or the leading edges of a delta wing. These are steady-state fields. On the other hand, in bluff-body flows, investigators use the term vortex shedding to imply alternate and dynamic shedding of large vortical structures. Since this paper is addressed to the community of aerodynamicists, we will conform with the established terminology. For the dynamic motions we will use the term "periodic vortex shedding."

Some interesting questions can be posed now. 1) What happens if the shedding edges remain normal to the oncoming stream but cease to be parallel to each other? This question was addressed in Refs. 16 and 17, and it was found that shedding occurs at frequencies varying with the local value of the width. 2) What happens as the angle of attack α in Fig. 1 increases? The latter case is the topic of the present investigation. Along this line of thought, the following specific questions can now be posed for a delta wing at high angles of attack:

1) Will the vortical structures detach periodically from the edges and shed in the wake of the wing?

2) Will vortices that align with the mean flow as shown in Fig. 1 be stable or could they engage in some periodic fluctuations?

3) If vortical structures detach, will they shed simultaneously as shown schematically in Fig. 3 or will they shed alternately, as shown in Fig. 4?

4) Will the axis of the detached vortex be parallel to the leading edge, will it be normal to the direction of the oncoming stream, or will it assume another orientation?

The first of the previous questions was investigated in Ref. 16 by the present authors. The occurrence of periodic vortex shedding downstream of a delta wing was documented there. On the last issue some information was reported by Ramberg,[20] who investigated the flow over an inclined finite cylinder. Ramberg discovered via flow visualization that it is possible for the axes of the vortices to be parallel to the axis of the inclined cylinder. Moreover, he found that near the windward free end of the cylinder the vortices are inclined in a direction that is neither parallel to the cylinder nor normal to the oncoming stream. In this paper, we describe our efforts to answer the previous questions. Evidence we provide is quite clear on some issues, but others may require more research.

III. Experimental Facilities

Experiments were conducted in the Virginia Polytechnic Institute (VPI) stability tunnel, the Engineering Science and Mechanics (ESM) wind tunnel, and the ESM water tunnel. Measurements were obtained with hot-wire anemometry and pressure transducers. The hot-wire equipment consisted of two DISA type 55D01 constant temperature anemometers and two 5-μ, tungsten-wire hot-wire probes. Endevco pressure transducers coupled with custom-made amplifiers were employed.

The VPI stability tunnel is a closed-circuit wind tunnel with a 6- $\times$ 6-ft test section, a turbulence level less than 0.07%, and a maximum attainable speed of almost 88 m/s. A special mechanism behind the model traverses the hot-wire probes in all three directions. The angle of attack of the wing can be varied between 30 and 80 deg and can be adjusted from the control room.

The signals were processed by a two-channel Hewlett Packard signal analyzer (HP 5420A). This equipment displays the response in both time and frequency domain, and for a two-channel input it provides the cross spectrum of the two signals, magnitude and phase.

The ESM wind tunnel is an open-circuit tunnel with a 0.508- $\times$ 0.508-m test section and is provided with a traversing system where the two hot-wire probes were mounted. Flow visualization tests were conducted in this tunnel using a humidifier, in conjunction with a laser system generating laser sheets. The flow at several stations over the wing was thus visualized. Flow visualization tests were also conducted in the ESM 0.254- $\times$ 0.305-m water tunnel.

Five geometrically similar delta wing models with a sweep angle of 76 deg were employed in this study. Their dimensions are given in Fig. 5. Model 1 is provided with three internal compartments not communicating with each other through which dye is supplied. The middle one communicates through a small hole right at the apex. The dye supplied through this compartment facilitates visualization of the vortex cores, whereas the dye supplied through the other two helps visualize the rolling up of the leading-edge shear layers. Models 2 and 3

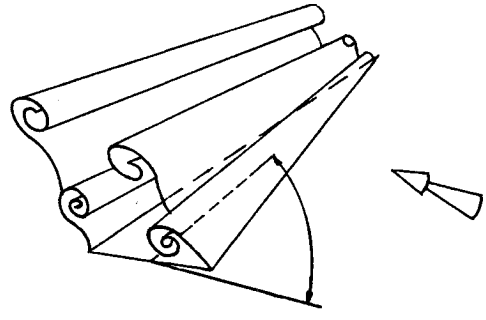

Fig. 4 Schematic of vortical structures shedding alternately over a delta wing at a large angle of attack.

were not instrumented. The latter was mounted on a balance system that allowed the measurement of unsteady components. Models 4 and 5 were instrumented with Endevco surface pressure transducers distributed along a line that runs underneath the estimated location of the leading-edge vortex core. Referring to Fig. 5, the dimensions of these models are: Model 4: $C = 0.345$ m, $S = 0.175$ m, $t = 16$ mm and Model 5: $C = 1$ m, $S = 0.521$ m, $t = 38$ mm. A total of seven transducers was used on each model. In the figure, the numbering of the first and the last ones is indicated.

All models were mounted on a sting via attachments at the center of the trailing edge. The attachments did not extend more than 20% upstream of the trailing edge on the windward side.

A schematic of the model in the tunnel showing the position of hot wires and the coordinate system is shown in Fig. 6. All coordinates are nondimensionalized with the wing chord length.

IV. Results and Discussion

In the preliminary phase of this effort, the delta wing model 2 was tested in the ESM wind tunnel at Reynolds numbers ranging from 3.9×10^4 to 1.72×10^5. As reported in Ref. 18, it was found that for angles of attack less than 36 deg the velocity spectra in the wake are totally void of any spikes, indicating the absence of any organized periodic shedding activity. As the angle of attack increases, periodic shedding suddenly appears and dominates the wake for all larger angles of attack. The phenomenon proved to be perfectly repeatable and very sensitive to angle-of-attack changes.

Tests were later repeated in the 6- × 6-ft stability tunnel with model 3 at Reynolds numbers ranging from 5.1×10^5 to 9.02×10^5. The results appear to be nearly independent of the Reynolds number. However, the sharp change of the character of the flow around the value of $\alpha = 37$ deg could not be reproduced. At lower Reynolds numbers, a change of just 1 deg in the angle of attack, from $\alpha = 36$ to 37 deg, was enough to generate unsteadiness in the wake. The phenomenon was repeatable, and no hysteresis was observed. For larger Reynolds numbers, it was found that unsteadiness sets in at a slightly lower angle of attack, namely, $\alpha = 35$ deg. Moreover, there was a hysteresis of a couple of degrees in producing or eliminating the dynamic phenomenon. It is possible that sec-

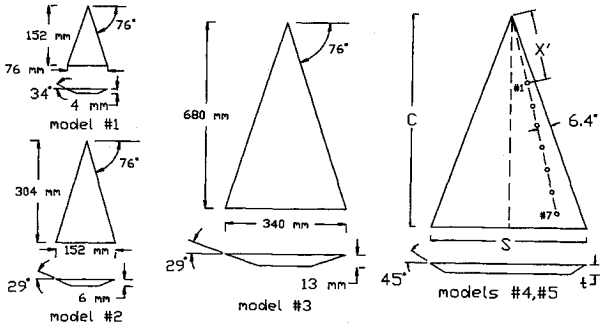

Fig. 5 Five delta wing models.

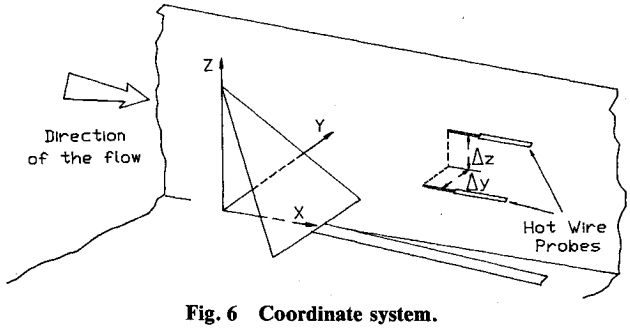

Fig. 6 Coordinate system.

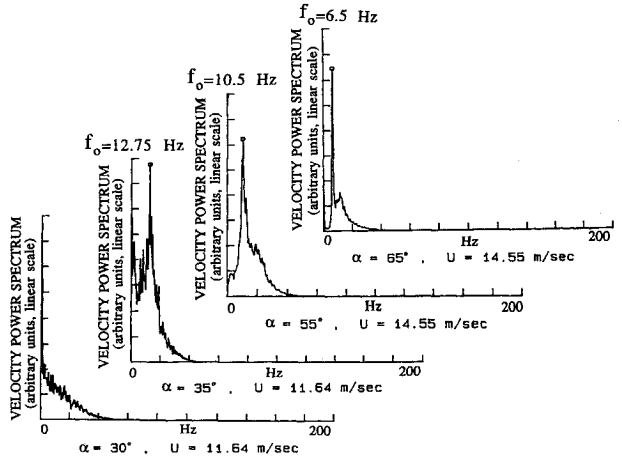

Fig. 7 Velocity spectra for the case of the delta wing.

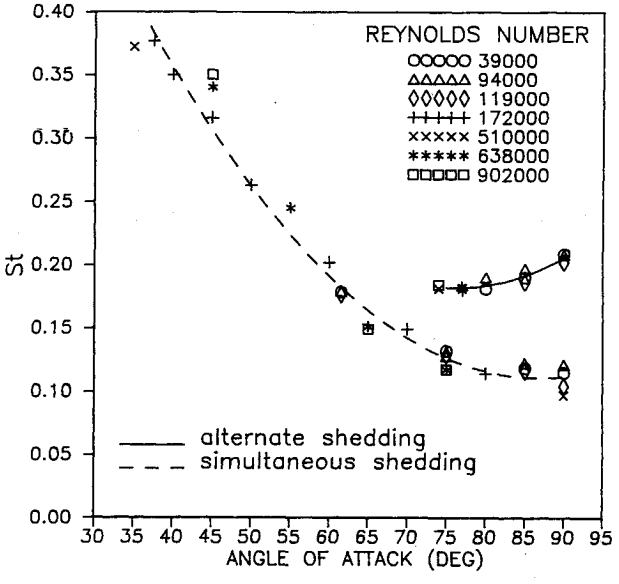

Fig. 8 Dimensionless frequency of shedding St ($= f \cdot S/U$ where f is the shedding frequency, S is the wing span, and U is the freestream velocity) as a function of the angle of attack for different Reynolds numbers. Lines represent a least-squares fit to the experimental data.

ondary separation that is controlled by the Reynolds number affects the onset of periodic vortex shedding. Figure 7 shows a few representative velocity spectra in the wake of the wing, obtained in the stability tunnel, for several velocities and angles of attack. Organized periodic behavior can be recognized in the form of a spike. More experimental data are provided in Ref. 16.

Further studies of the Strouhal number behavior for the entire range of angles of attack revealed a rather interesting behavior as shown in Fig. 8. As the angle of attack increases, the Strouhal number decreases and seems to be leveling off at around 0.10–0.13. And then near $\alpha = 70$ deg a second, higher frequency appears in the spectrum. Evidence that these frequencies represent some form of vortex shedding is the fact that their magnitude is proportional to the velocity. In other words, they increase linearly with the freestream speed. It is very important to note here that data in Fig. 8 were obtained in two different tunnels with different characteristics. Yet they collapse along well-defined curves.

A more careful examination revealed that for $\alpha > 70$ deg, the two frequencies correspond to the two modes of shedding, namely, simultaneous shedding and alternate shedding, respectively. This was discovered by sampling the wake with two

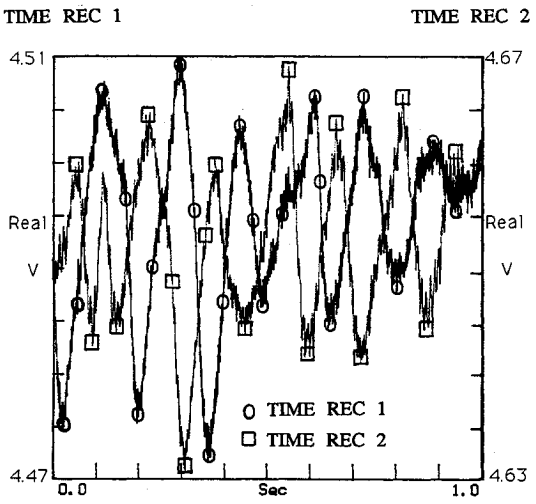

Fig. 9 Time records obtained with two hot wires positioned in the wake of a delta wing at $\alpha = 74$ deg ($Re = 3 \times 10^5$).

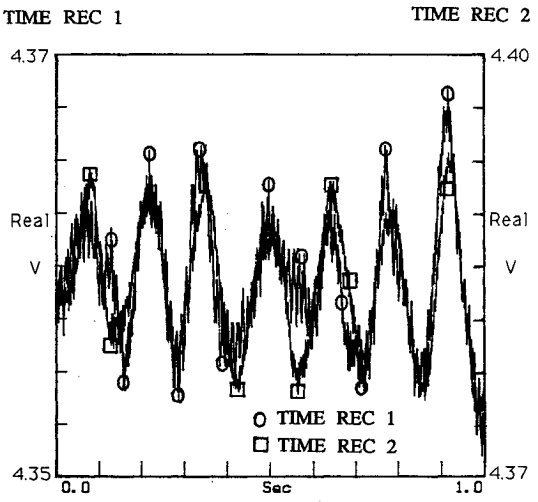

Fig. 10 Time records obtained with two hot wires positioned in the wake of a delta wing at $\alpha = 60$ deg ($Re = 3 \times 10^5$).

wires, symmetrically positioned about the plane of symmetry of the wing. Time records obtained from hot wires positioned at $(x, y, z) = (1.5, \pm 0.3, 0.5)$ in the VPI stability tunnel are displayed in Fig. 9. These data were obtained at a Reynolds number of 3×10^5 and an angle of attack of $\alpha = 74$ deg. A phase difference of 180 deg clearly indicates alternate vortex shedding. Data obtained in the same way at a lower angle of attack, $\alpha = 60$ deg, with the hot wires positioned at $(x, y, z) = (1, 7, \pm 0.3, 0.4)$ and at a Reynolds number of $Re = 3 \times 10^5$ are presented in Fig. 10. The traces now are in phase, indicating that the vortices are shed simultaneously.

Our data-processing method displays results in a frequency domain as well. It is also possible, by triggering the signals, to obtain ensemble averages. The phase of the cross spectrum then is essentially a statistical mean of the phase difference between the two signals. This method was employed throughout this investigation. In Fig. 11, we show the cross spectrum of the two hot-wire signals in the case of $\alpha = 60$ deg. The two hot wires are placed at $z = 0.4$. There is only one spike, corresponding to the shedding frequency (6.75 Hz) at that freestream velocity (12.75 m/s). The phase of the cross spectrum at this frequency is the phase difference between the two signals (-2.7 deg). Within an experimental error, these two signals are in phase. This indicates that at this angle of attack only simultaneous shedding takes place. Experiments at several angles of attack indicate that in the range $\alpha = 40$–70 deg no alternate shedding occurs. On the other hand, at angles of attack larger than 70 deg, both shedding modes (simultaneous and alternate) exist. Figure 12 shows the cross spectrum at an angle of attack of $\alpha = 74$ deg ($z = 0.5$). Two spikes are present here. The first, at the lower frequency (6.25 Hz), corresponds to a phase difference of the signals of -2.5 deg (very close to 0 deg), whereas the second, at the high frequency (10.25 Hz), corresponds to a phase difference of 178.8 deg (very close to 180 deg), indicating alternate shedding. The relative magnitudes of the spikes indicate that the simultaneous mode dominates. Moving the hot-wire probes closer to the trailing edge, for the same angle of attack ($\alpha = 74$ deg), we observed that the relative magnitude of the two modes is about the same. Cross spectra obtained at angles of attack ranging between 70 and 90 deg (not shown here) prove that in this range the two modes coexist, with the alternate mode gaining relative importance as we move closer to the trailing edge ($z \to 0$, keeping x and y constant).

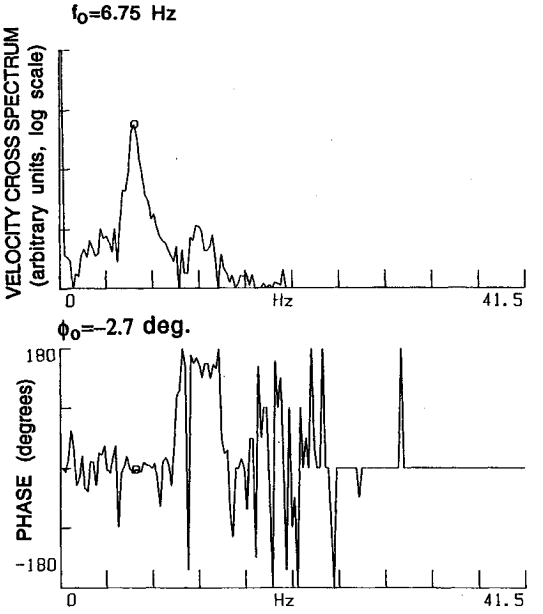

Fig. 11 Magnitude and phase of cross spectrum of two hot wires positioned at $(x_1, y_1, z_1) = (1.7, 0.3, 0.4)$ and $(x_2, y_2, z_2) = (1.7, -0.3, 0.4)$ for $\alpha = 60$ deg.

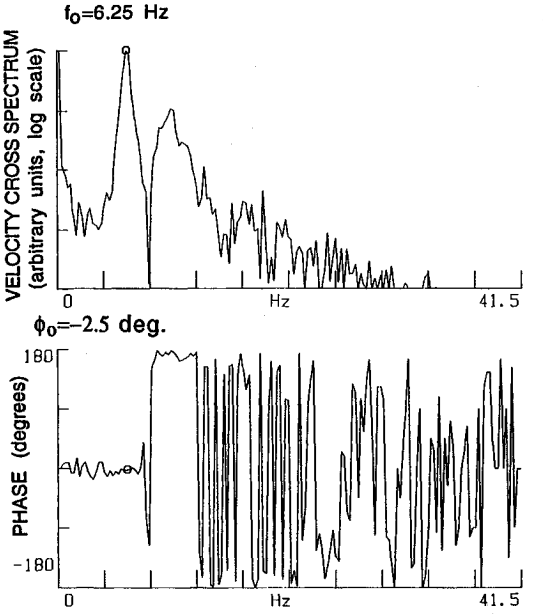

Fig. 12 Magnitude and phase of cross spectrum of two hot wires positioned at $(x_1, y_1, z_1) = (1.5, 0.3, 0.5)$ and $(x_2, y_2, z_2) = (1.5, -0.3, 0.5)$ for $\alpha = 74$ deg.

The results shown in Fig. 8 were calculated in terms of the statistical mean of the frequencies measured. Based on the phase information between the signals of two symmetrically positioned wires, we were able to distinguish the two modes of shedding. This figure indicates that no shedding is present below $\alpha = 35$ deg. At about this value, simultaneous shedding originates, characterized by a Strouhal number that decreases monotonically with the angle of attack. At about $\alpha = 70$ deg, the mode of alternate shedding also appears. For higher angles of attack, the two modes coexist.

It is of interest to note here that in our preliminary studies at moderate angles of attack we were unable to measure any oscillation in the rolling moment measured on the line by a balance system. The pressure and velocity data presented here indicate that for angles of attack less than 70 deg the organized oscillations are indeed symmetric about the plane of symmetry.

For angles of attack larger than 35 deg, a phenomenon that dominates the flow in the vicinity of the wing is vortex breakdown. To explore whether this phenomenon is related to the unsteady effects detected in the wake of the wing, we measured surface pressures along ports 1–7 (Fig. 5). For angles of attack less than 35 deg, the spectra of these sensors contain no discernible spikes. As the angle of attack increases, a certain organization appears first near the trailing edge of the wing and starts creeping up with the angle of attack. The frequencies measured are listed in Table 1. These frequencies are much larger than shedding frequencies and are not in any way related to the latter. Typical examples of pressure spectra are displayed in Fig. 13. It is very significant to note that these frequencies were detected again in two different tunnels, and the data were reduced by different hardware and software.

These organized motions were detected over areas of the wing and in the domain of angles of attack for which vortex breakdown was observed. We are therefore led to believe that we have captured the trace of some organized activity of vortex breakdown. Faler and Leibovich[21] observed organized periodic activity in columnar vortices breaking down in a tube. It is very hard to choose the characteristic lengths and velocities to reduce the frequencies in the two cases. For a crude comparison we reduced our data with the half-span and the core axial velocity and the Faler and Leibovich data with the inlet diameter of the tube and the maximum axial velocity. The two figures are 0.18 and 0.58, respectively. However, we believe that the two unsteady phenomena are not identical because the Faler and Leibovich flow involves a laminar breakdown of the bubble type, whereas in our case the flow develops a fully random pattern.

At angles of attack larger than 55 deg, all pressure sensors indicate a much lower frequency that coincides with the wake frequency reported earlier. In this range vortex breakdown has reached the apex and no longer plays a role in the development of the flow. It is believed that in this range the vortical structures are shed uniformly from the surface of the wing, and thus all sensors, either on the surface or in the wake, pick up the same characteristic frequency, just as in the case of two-dimensional periodic vortex shedding over a bluff body. Typical examples are shown in Fig. 14.

Table 1 Dominant frequencies in the surface pressure power spectra for different angles of attack and Reynolds numbers

Angle of attack α, deg	Reynolds no. $Re/10^5$	Frequency f, Hz	Strouhal no. $St, f \cdot S/U$
37.5	2.1	47.25	0.89
39	2.1	45.5	0.86
47	2.1	32.25	0.61
47	2.7	41.5	0.61
36	9.3	24.5	0.9
38	9.3	23.0	0.84
40	9.3	24.0	0.88
36	16	44.5	0.94
38	16	42.0	0.88
40	16	39.0	0.82

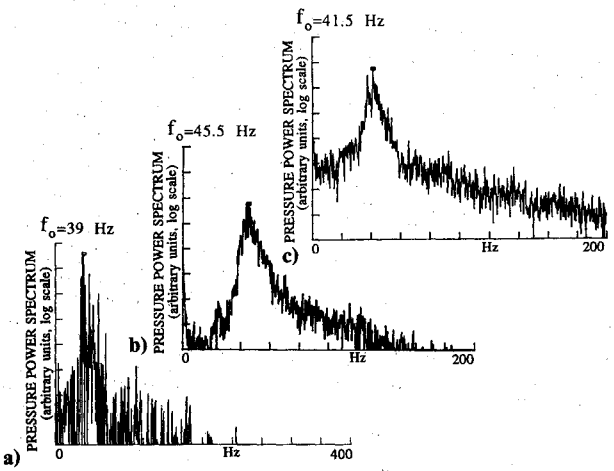

Fig. 13 Pressure power spectra: a) $Re = 1.6 \times 10^6$ (stability tunnel), $\alpha = 40$ deg, pressure port 7, $x'/C = 0.85$; b) $Re = 2.1 \times 10^5$ (ESM tunnel), $\alpha = 39$ deg, port 7, $x'/C = 0.92$; and c) $Re = 2.7 \times 10^5$ (ESM tunnel), $\alpha = 47$ deg, port 7, $x'/C = 0.92$.

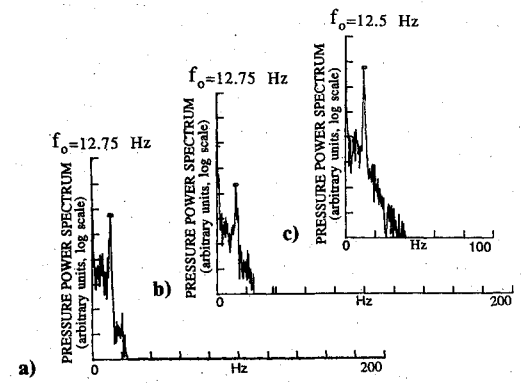

Fig. 14 Pressure power spectra for $Re = 2.7 \times 10^5$, $\alpha = 63$ deg, pressure ports 1, 6, and 7 with $x'/C = 0.37$, 0.83, and 0.92, respectively.

To examine the velocity with which shed vortices drift downstream, it is necessary to position two wires in the streamwise direction. With one wire fixed and the other traversing in the x direction along the same y and z position, it was possible to estimate the drifting velocity. The measurements were conducted at $\alpha = 60$ deg, where we know that only simultaneous shedding takes place. It was observed that wave packets propagate with nearly constant velocities at a fixed elevation. For two wires positioned at a distance Δx apart, the packet speed can be determined in terms of the phase difference $\Delta\phi$ of the two signals and the shedding frequency f from the formula

$$U_p = 2\pi f \Delta x / \Delta\phi$$

This velocity is an average of the phase speed over the distance Δx. Table 2 lists the packet velocities at two different elevations z_1 and z_2 corresponding to two different spanwise locations y_1 and y_2, such that the points (x_1, y_1, z_1) and (x_1, y_2, z_2) lie on the projection of the wing's leading edge on the plane $x = x_1$. From this table, it is obvious that the packet velocity at locations closer to the apex is larger than that at locations closer to the trailing edge. Therefore, since different parts of the shed vortex axis are moving with different speeds, the relative orientation of the wave with respect to the wing changes as the disturbance is carried downstream. To estimate this orientation and its change, the following procedure was followed. First we measured the drifting velocity at several elevations z between z_1 and z_2, and by fitting a curve we obtained a continuous variation of U_p vs z. Then we fixed one of the probes at a position (x_0, y_0, z_0) and moved the second,

Table 2 Drifting velocities U_p of two different elevations—Z_1 and Z_2 — for a freestream velocity of $U = 12.75$ m/s and an angle of attack $\alpha = 60$ deg ($x_1 = x_2 = 1.0$)

Δx, m	U_p, m/s
$z_1 = 0.7$:	
0.152	9.987
0.229	10.289
0.305	9.66
—	—
$z_2 = 0.1$:	
0.152	8.35
0.229	7.76
0.305	7.18
0.381	7.576

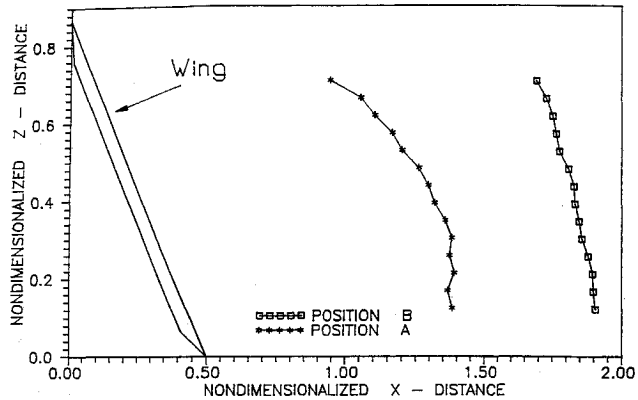

Fig. 15 Instantaneous positions of the wave fronts of vortices shed over a wing at an angle of attack of $\alpha = 60$ deg.

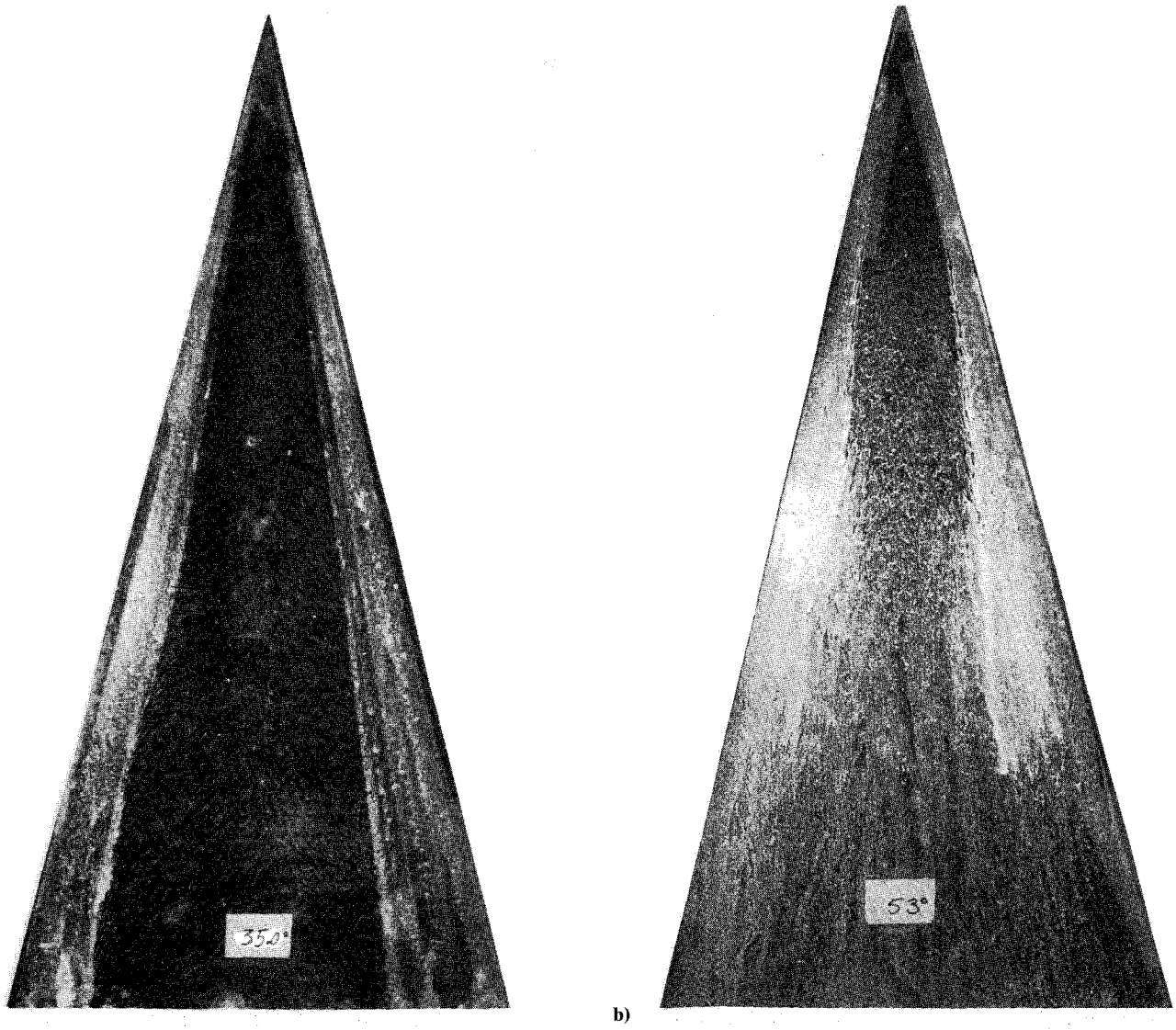

a) b)

Fig. 16 Skin friction lines for two different angles of attack.

keeping $x = x_0$, so that the line segment connecting the two probes always lay on the leading edge's projection on the plane $x = x_0$. Measuring the phase difference between the two signals and knowing the local value of the drifting velocity, we were able to calculate the orientation of the drifting vortex at two different x_0. The results are given graphically in Fig. 15. Position A corresponds to $x_0 = 0.9$ and position B to $x_0 = 1.7$. In the figure the data are projected on a plane $y = \text{const}$. The tendency of the flowfield to straighten up the vortex is obvious.

Efforts in visualizing the flow provided some evidence to confirm the results obtained through velocity measurements. In Fig. 16 we display skin friction lines for two different angles of attack. For $\alpha < 35$ deg, the coherent leading-edge vortices generate a powerful spanwise pressure gradient, which in turn induces separation and a second set of counter-rotating vortices. The line of secondary separation and therefore the region where the skin friction lines converge are clearly defined (Fig. 16a). This line is confined closer to the apex as the angle

Fig. 17 Flow visualization for an angle of attack of 31.5 deg.

Fig. 18 Flow visualization for an angle of attack of 53 deg.

of attack increases (Fig. 16b). This indicates that the activity over the wing is changing character. A well-defined line of secondary separation indicates that the vortex is attached to the leading edge and that this region is void of any organized periodic activity.

The flow was also visualized by seeding the field with humidity and employing laser sheet cuts. The film was exposed for a few seconds, and therefore an average of the motion was obtained. At low angles of attack, the leading-edge vortices are fixed and their core is clearly indicated by a dark circle, as shown in Fig. 17. However, at higher angles of attack, the flow must engage in some periodic activity that in the average appears as blurred shadows in Fig. 18.

A known and well-established case of vortex shedding is that of a rectangular flat plate placed normal to the flow. Visualization of this field indicated that averaging of the flow displays the same behavior with that of the lower part over the wing of Fig. 18. In both cases, there is no clear core of the vortex. On the other hand, the core of the leading-edge vortex in Fig. 17 is well defined. These observations, in conjunction with the information we get from the skin friction line pattern (Fig. 16b) for $\alpha = 53$ deg, lead to the conclusion that at the upper almost 20% of the wing the leading-edge vortices stay attached to the wing and no shedding takes place. But over the rest of the wing the vortices lift off and start shedding periodically. From pressure and velocity data we know that this activity is symmetric. However, it is not yet clear whether this dynamic motion involves the simultaneous detachment of vortical structures over the entire edge of the wing, in a pattern similar to two-dimensional periodic vortex shedding, or whether the vortical structures align with the stream and undulate in heave.

Flow visualization tests were also conducted in the ESM water tunnel. Red dye was released very near the apex of the model, consistently seeding the core of the vortex. Two blue dye ports were located near the edge and at about 0.2 chords from the apex. These frames are not included here due to lack of space. For small angles of attack, the blue dyes follow the familiar helical pattern, wrapping around the red dye, which allows us to visualize the free shear layer. For $\alpha = 35$ deg, the structure remains well behaved until the trailing edge of the wing. For $\alpha = 55$ deg, the red dye starts off straight and soon indicates evidence of the onset of vortex breakdown. Farther down along the wing, near the region of the blue dye ports, the flow structure is changing character. The axial motion of the flow is suppressed. The blue dye pattern is incoherent and definitely departs from the conical geometry.

V. Conclusions

The flow over a delta wing with a sweep angle of 76 deg induces vortex shedding at angles of attack above 35 deg. At or below this angle, the two leading-edge vortices remain attached on the wing all of the way from the apex to the trailing edge. Above this angle, two regions can be distinguished on the wing: one starting from the apex, where the vortices stay attached; and the second confined to the aft part of the wing, where the vortices lift off the wing surface and are shed.

In the range of $35 < \alpha < 70$ deg, vortices are shed simultaneously from the leading edges. However, for $\alpha > 70$ deg, a second shedding mode at a higher frequency enters the picture. Some evidence was provided indicating that alternate shedding occurs near the trailing edge and spreads toward the apex as the angle of attack increases, probably dominating shedding for $\alpha = 90$ deg. In all cases, the shedding frequency is dependent on the angle of attack. The dependence is nonlinear.

Acknowledgments

The support of the Air Force Office of Scientific Research, Grant AFOSR-89-0283, H. E. Helin, monitor, is gratefully acknowledged. The support of NATO Grant 0441/87 has helped with international travel for this cooperative research program.

References

[1]Berger, E. W., and Willie, R., "Periodic Flow Phenomena," *Annual Review of Fluid Mechanics,* Vol. 4, June 1972, pp. 313-340.

[2]Cermak, J. E., "Aerodynamics of Buildings," *Annual Review of Fluid Mechanics,* Vol. 8, Jan. 1976, pp. 75-106.

[3]Sarpkaya, T., "Vortex-Induced Oscillation," *Journal of Applied Mechanics,* Vol. 46, March 1979, pp. 241-258.

[4]Griffin, D. M., "Universal Similarity in the Wakes of a Stationary and Vibrating Bluff Structures," *Journal of Fluid Engineering,* Vol. 103, March 1981, pp. 52-58.

[5]Saffman, P. G., and Schatzman, J. C., "An Inviscid Model for the Vortex Street Wake," *Journal of Fluid Mechanics,* Vol. 122, Sept. 1982, pp. 467-486.

[6]Zdravkovich, M., *Flow Past Cylinders,* Springer-Verlag, New York, 1987.

[7]Barbi, C., Favier, D. P., Maresca, C. A., and Telionis, D. P., "Vortex Shedding and Lock-On of Circular Cylinder in Oscillatory Flow," *Journal of Fluid Mechanics,* Vol. 170, Sept. 1986, pp. 527-544.

[8]Malcom, G. N., and Schiff, L. B., "Recent Developments in Rotary-Balance Testing of Fighter Aircraft Configurations, at NASA Ames Research Center," AGARD-CP-386, May 1985, pp. 18-1-18-25.

[9]Brandon, J. M., and Shah, G. H., "Effect of Large Amplitude Pitching Motion on the Unsteady Aerodynamic Characteristics of Flat-Plate Wings," AIAA Paper 88-4331, Aug. 1988.

[10]LeMay, S. P., Batill, S. M., and Nelson, R. C., "Leading Edge Vortex Dynamics on a Pitching Delta Wing," AIAA Paper 88-2559, June 1988.

[11]Ayoub, A., and McLachlan, B. G., "Slender Delta Wing at High Angles of Attack—A Flow Visualization Study," AIAA Paper 87-1230, June 1987.

[12]Ericcson, L. E., and Reding, J. P., "Fluid Dynamics of Unsteady Separated Flow, Part II: Lifting Surfaces," *Progress in Aerospace Sciences,* Vol. 24, No. 4, 1987, pp. 249-356.

[13]Ericcson, L. E., and Reding, J. P., "Asymmetric Vortex Shedding from Bodies of Revolution," *Tactical Missile Aerodynamics,* Progress in Astronautics and Aeronautics, edited by M. J. Hemsch and J. N. Nielsen, Vol. 104, AIAA, New York, 1986, pp. 243-296.

[14]Gaster, M., "Vortex Shedding from Slender Cones," *Proceedings of IUTAM Symposium on Recent Research on Unsteady Boundary Layers* (Laval Univ., Quebec, Canada), Vol. II, May 24–28, 1971, pp. 1499–1534.

[15]Gaster, M., and Ponsford, P. J., "The Flows over Tapered Flat Plates Normal to the Stream," *Aeronautical Journal,* Vol. 88, No. 857, May 1984, pp. 206–212.

[16]Rediniotis, O. K., Stapountzis, H., and Telionis, D. P., "Vortex Shedding over Nonparallel Edges," Virginia Polytechnic Inst. and State Univ., Engineering Rept. VPI-E-88-39, Blacksburg, VA, Dec. 1988.

[17]Klute, S., Rediniotis, O., Stapountzis, H., and Telionis, D., "Vortex Shedding over Non-Parallel Edges," *Proceedings of the Third International Congress of Fluid Mechanics* (Cairo, Egypt), Vol. II, Jan. 1990, pp. 587–601.

[18]Rediniotis, O. K., Stapountzis, H., and Telionis, D. P., "Vortex Shedding over Delta Wings," *AIAA Journal,* Vol. 28, No. 5, 1990, pp. 944–946.

[19]Roshko, A., "On the Drag and Shedding Frequency of Two-Dimensional Bluff Bodies," NACA TN 3169.

[20]Ramberg, S. E., "The Effects of Yaw and Finite Length upon the Vortex Wakes of Stationary and Vibrating Circular Cylinders," *Journal of Fluid Mechanics,* Vol. 128, March 1983, pp. 81–107.

[21]Faler, J. H., and Leibovich, S., "An Experimental Map of the Internal Structure of a Vortex Breakdown," *Journal of Fluid Mechanics,* Vol. 86, May 1978, pp. 313–335.